Molecular Physics, 2015
Vol. 113, Nos. 13–14, 1843–1857, http://dx.doi.org/10.1080/00268976.2015.1017018

INVITED ARTICLE

Chem1D: a software package for electronic structure calculations on one-dimensional systems

Caleb J. Ball* and Peter M.W. Gill

Research School of Chemistry, Australian National University, Canberra, Australia

(*Received 15 December 2014; accepted 5 February 2015*)

We present a preliminary version of a software package, CHEM1D, that performs molecular orbital calculations on one-dimensional atoms and molecules using the unadorned Coulomb operator $1/|x_1 - x_2|$. We describe methods for computing the necessary one- and two-electron integrals and outline the overall structure of the package. We use CHEM1D to perform calculations on a set of small molecules and show that one-dimensional chemistry differs in a number of interesting ways from three-dimensional chemistry.

Keywords: *ab initio*; molecular orbital; wave function; one-dimensional molecule; linear molecules

1. Introduction

One-dimensional (1D) chemistry is an exciting and emerging field. Many quasi-linear systems have been studied experimentally: carbon nanotubes [1–5], organic conductors [6–10], transition metal oxides [10], edge states in quantum Hall liquids [11–13], semiconductor heterostructures [14–18] and confined atomic gases [19–21]. Likewise, a number of theoretical studies of quasi-linear systems have been published, such as those by Burke and co-workers [22,23] and Herschbach and co-workers [24–26].

Almost all previous work has been based on Hamiltonians with softened Coulomb operators.

López-Castillo [27] has performed an extensive semiclassical study of the 1D hydrogen molecule using the unadorned $1/|x_1 - x_2|$ operator. The present authors in collaboration with Loos have recently reported a quantum study [28], which also uses the $1/|x_1 - x_2|$ operator throughout, that focuses on the chemical ramifications.

This formulation allows us to investigate the behaviour of normal electrons that are strictly confined on a line. Such systems were first treated in the seminal work by Loudon [29] on the 1D hydrogen atom. Unfortunately, the literature on this topic has been fraught with controversy [30–36] and a number of theoretical starting points have been proposed.

The fundamental difficulty is the fact that the Coulomb operator in 1D, unlike in three dimensions [37], is not self-adjoint. As a consequence, in order to evaluate the energy, it is necessary to construct a suitable extension or, equivalently, impose a set of boundary conditions. Oliveira and Verri have shown [38] that many extensions are possible but we have chosen the Dirichlet boundary condition, which requires the wave function to vanish when two particles touch. Later work by Oliveira and co-workers [39,40] has shown that this physically appealing choice arises naturally when considering electrons that are gradually confined to the line by a sequence of increasingly small cylinders but we emphasise that our numerical results depend critically on this choice.

The Dirichlet choice has three consequences. First, as Núñez-Yépez and co-workers have argued [41,42], the electrons and nuclei become mutually impenetrable which has far-reaching implications for 1D chemistry. Second, the energy is independent of the spin state, allowing us to assume (for example) that all electrons are spin-up. Third, by the exclusion principle, no orbital may contain more than one electron.

In this article, we describe the software package that we developed for our recent work [28]. In Section 2, we describe the underlying theory and, particularly, our two-electron integral methodology. Section 3 sketches the overall structure of our program and Section 4 presents and discusses some new results that it has yielded.

2. Theory

2.1. Notation

Within the Dirichlet choice, particles that are confined strictly to a line are impenetrable to each other. As a result, the electrons are trapped in the regions of space ('domains') between adjacent nuclei. A 1D molecule with N nuclei has an infinite domain (domain 0) to the left of the molecule, $N - 1$ finite domains (domains 1, 2, ..., $N - 1$) between adjacent nuclei, and another infinite domain (domain N) to the right of the molecule.

* Corresponding author. Email: caleb.ball@anu.edu.au

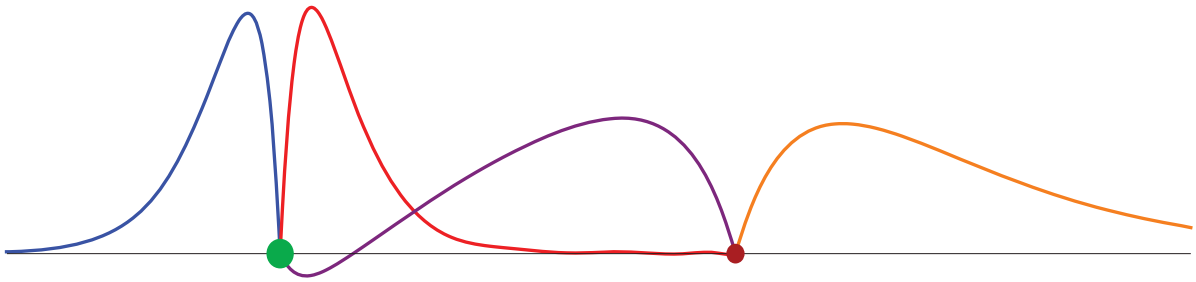

Figure 1. The four singly occupied orbitals of the molecule $_1Li_2H_1$. The green dot represents the Li nucleus, the red dot the H nucleus and each coloured line is an occupied orbital.

To describe a state of a 1D molecule, one specifies the nuclei and their positions A_p ($p = 1, \ldots, N$), the number of electrons in each domain and the orbitals they occupy. CHEM1D currently treats only ground states and so, henceforth, we will assume that the occupied orbitals in each domain are those of lowest energy.

Our notation is straightforward. For example, the $_1Li_3He_1H_2Be_2$ molecule consists of four nuclei and nine electrons. There is one electron in domain 0 to the left of the Li nucleus, three in domain 1 between the Li and He nuclei, one in domain 2 between the He and H nuclei, two in domain 3 between the H and Be nuclei and two in domain 4 to the right of the Be nucleus. As mentioned above, these electrons singly occupy the lowest energy orbitals of their associated domains.

A graphical representation of the $_1Li_2H_1$ molecule and its occupied orbitals is shown in Figure 1.

2.2. *Basis sets*

For this work, we have developed a set of basis functions to describe the orbitals. A basis function $\mathbf{F}^p_\mu$ has index μ and resides entirely in domain p. When the domain superscript is redundant it is omitted. It is easy to see that the basis function pair $(\mathbf{F}^p_\mu \mathbf{F}^q_\nu|$, with $p \neq q$, must necessarily vanish everywhere.

In domain 0, we have a set of normalised exponentials

$$\mathbf{L}_\mu(x) = 2\mu^3\alpha^{3/2}(A_1 - x)\exp[-\mu^2\alpha(A_1 - x)] \qquad (1)$$

in domain N, we have an analogous set of exponentials

$$\mathbf{R}_\mu(x) = 2\mu^3\alpha^{3/2}(x - A_N)\exp[-\mu^2\alpha(x - A_N)] \qquad (2)$$

and, in the finite domains, we have even polynomials

$$\mathbf{E}^p_\mu(x) = \sqrt{\frac{2/\pi^{1/2}}{R}\frac{\Gamma(2\mu + 3/2)}{\Gamma(2\mu + 1)}}\,(1 - z^2)^\mu \qquad (3)$$

and odd polynomials

$$\mathbf{O}^p_\mu(x) = \sqrt{\frac{4/\pi^{1/2}}{R}\frac{\Gamma(2\mu + 5/2)}{\Gamma(2\mu + 1)}}\,z(1 - z^2)^\mu, \qquad (4)$$

where $z = (A_p + A_{p+1} - 2x)/(A_p - A_{p+1})$, $R = A_{p+1} - A_p$ and Γ is the Gamma function. We include only positive integer μ to ensure that the orbitals vanish at the nuclei.

All of the necessary one-electron integrals can be found in closed form and we list the relevant formulae below. We also present a discussion of the algorithms we have developed for evaluating the required two-electron quantities. We use chemist's notation [43] throughout.

2.3. *One-electron integrals*

Define $\hat{T} = -\nabla^2/2$, $\hat{V}_p = |x - A_p|^{-1}$, $\zeta = \mu^2 + \nu^2$, $\eta = \lambda^2 + \sigma^2$ and

$$G(x, y) = \frac{\Gamma(x + y)}{\sqrt{\Gamma(2x)\,\Gamma(2y)}}. \qquad (5)$$

2.3.1. *Overlap integrals*

All overlap integrals vanish except the following

$$(\mathbf{L}_\mu|\mathbf{L}_\nu) = (\mathbf{R}_\mu|\mathbf{R}_\nu) = (2\mu\nu/\zeta)^3 \qquad (6)$$

$$\left(\mathbf{E}^p_\mu|\mathbf{E}^p_\nu\right) = \frac{G(\mu + 1/2, \nu + 1/2)}{G(\mu + 3/4, \nu + 3/4)} \qquad (7)$$

$$\left(\mathbf{O}^p_\mu|\mathbf{O}^p_\mu\right) = \frac{G(\mu + 1/2, \nu + 1/2)}{G(\mu + 5/4, \nu + 5/4)}. \qquad (8)$$

2.3.2. *Kinetic integrals*

All kinetic energy integrals vanish except the following

$$\frac{(\mathbf{L}_\mu|\hat{T}|\mathbf{L}_\nu)}{(\mathbf{L}_\mu|\mathbf{L}_\nu)} = \frac{(\mathbf{R}_\mu|\hat{T}|\mathbf{R}_\nu)}{(\mathbf{R}_\mu|\mathbf{R}_\nu)} = \frac{\alpha^2\mu^2\nu^2}{2} \qquad (9)$$

$$\frac{\left(\mathbf{E}_\mu^p|\hat{T}|\mathbf{E}_\nu^p\right)}{(\mathbf{E}_\mu^p|\mathbf{E}_\nu^p)} = \frac{4\mu\nu(\mu+\nu+1/2)}{(\mu+\nu)(\mu+\nu-1)}\frac{1}{R^2} \tag{10}$$

$$\frac{\left(\mathbf{O}_\mu^p|\hat{T}|\mathbf{O}_\nu^p\right)}{(\mathbf{O}_\mu^p|\mathbf{O}_\nu^p)} = \frac{12\mu\nu(\mu+\nu+3/2)}{(\mu+\nu)(\mu+\nu-1)}\frac{1}{R^2}, \tag{11}$$

where $R = A_{p+1} - A_p$.

2.3.3. Nuclear-attraction integrals

All nuclear-attraction integrals vanish except

$$\frac{(\mathbf{L}_\mu|\hat{V}_p|\mathbf{L}_\nu)}{(\mathbf{L}_\mu|\mathbf{L}_\nu)} = \frac{(\zeta\alpha R_p)^3}{R_p}U(3,3,\zeta\alpha R_p) \quad (R_p = A_p - A_1) \tag{12}$$

$$\frac{(\mathbf{R}_\mu|\hat{V}_p|\mathbf{R}_\nu)}{(\mathbf{R}_\mu|\mathbf{R}_\nu)} = \frac{(\zeta\alpha R_p)^3}{R_p}U(3,3,\zeta\alpha R_p) \quad (R_p = A_N - A_p) \tag{13}$$

$$\frac{\left(\mathbf{E}_\mu^q|\hat{V}_p|\mathbf{E}_\nu^q\right)}{(\mathbf{E}_\mu^q|\mathbf{E}_\nu^q)} = \frac{1}{|R_p|}F\left(1,\frac{1}{2},\mu+\nu+\frac{3}{2},\frac{a^2}{R_p^2}\right) \quad (R_p = |A_q + a - A_p|) \tag{14}$$

$$\frac{(\mathbf{O}_\mu^q|\hat{V}_p|\mathbf{O}_\nu^q)}{(\mathbf{O}_\mu^q|\mathbf{O}_\nu^q)} = \frac{1}{|R_p|}F\left(1,\frac{3}{2},\mu+\nu+\frac{5}{2},\frac{a^2}{R_p^2}\right) \quad (R_p = |A_q + a - A_p|) \tag{15}$$

$$\frac{(\mathbf{E}_\mu^q|\hat{V}_p|\mathbf{O}_\nu^q)}{(\mathbf{O}_\mu^q|\mathbf{O}_\nu^q)} = \frac{1}{|R_p|}F\left(1,\frac{3}{2},\mu+\nu+\frac{5}{2},\frac{a^2}{R_p^2}\right)\frac{a/R_p}{\sqrt{4\mu+3}} \quad (R_p = |A_q + a - A_p|), \tag{16}$$

where U is the confluent hypergeometric function [44], F is the Gauss hypergeometric function [44] and $a = (A_{q+1} - A_q)/2$.

2.4. Two-domain two-electron integrals

Antisymmetrised ('double bar') electron repulsion integrals (ERIs) quantify interactions between an electron in domain p and another in domain q. If $p \neq q$, we have

$$\begin{aligned}\left(\mathbf{F}_\mu^p\mathbf{F}_\nu^p||\mathbf{F}_\lambda^q\mathbf{F}_\sigma^q\right) &= \left(\mathbf{F}_\mu^p\mathbf{F}_\nu^p|\mathbf{F}_\lambda^q\mathbf{F}_\sigma^q\right) - \left(\mathbf{F}_\mu^p\mathbf{F}_\lambda^q|\mathbf{F}_\nu^p\mathbf{F}_\sigma^q\right)\\ &= \left(\mathbf{F}_\mu^p\mathbf{F}_\nu^p|\mathbf{F}_\lambda^q\mathbf{F}_\sigma^q\right)\end{aligned} \tag{17}$$

and there are three cases: (1) both domains are infinite; (2) one domain is infinite and the other is finite; (3) both domains are finite.

2.4.1. Infinite/infinite domains

If we let $\zeta = \mu^2 + \nu^2$, $\eta = \lambda^2 + \sigma^2$ and $R = A_N - A_1$, then

$$\begin{aligned}\frac{(\mathbf{L}_\mu\mathbf{L}_\nu|\mathbf{R}_\lambda\mathbf{R}_\sigma)}{(\mathbf{L}_\mu|\mathbf{L}_\nu)(\mathbf{R}_\lambda|\mathbf{R}_\sigma)} = \frac{\alpha\zeta\eta}{2(\zeta-\eta)^5}\Bigg(&\frac{1}{2}[5(\zeta+\eta)(\zeta-\eta)^3\\ &- 3(\zeta+\eta)^3(\zeta-\eta) - 2R\alpha\zeta\eta(\zeta-\eta)^3]\\ &- \zeta^2\eta^2\big[12 - 6R\alpha(\zeta-\eta)\\ &+ (R\alpha(\zeta-\eta))^2\big]U(1,1,R\alpha\zeta) + \zeta^2\eta^2\\ &\times\left[12 + 6R\alpha(\zeta-\eta) + (R\alpha(\zeta-\eta))^2\right]\\ &\times U(1,1,R\alpha\eta)\Bigg)\end{aligned} \tag{18}$$

or, in the limiting case where $\zeta = \eta$,

$$\begin{aligned}\frac{(\mathbf{L}_\mu\mathbf{L}_\nu|\mathbf{R}_\lambda\mathbf{R}_\sigma)}{(\mathbf{L}_\mu|\mathbf{L}_\nu)(\mathbf{R}_\lambda|\mathbf{R}_\sigma)} = \frac{\alpha\zeta}{120}\big(&24 - 6R\alpha\zeta + 2(R\alpha\zeta)^2\\ &- (R\alpha\zeta)^3 + (R\alpha\zeta)^4\\ &- (R\alpha\zeta)^5U(1,1,R\alpha\zeta)\big).\end{aligned} \tag{19}$$

When $R = 0$ (i.e. for atomic calculations), these two formulae reduce to

$$\begin{aligned}\frac{(\mathbf{L}_\mu\mathbf{L}_\nu|\mathbf{R}_\lambda\mathbf{R}_\sigma)}{(\mathbf{L}_\mu|\mathbf{L}_\nu)(\mathbf{R}_\lambda|\mathbf{R}_\sigma)} = \frac{\alpha\zeta\eta}{2(\zeta-\eta)^5}\Bigg((\zeta^2-\eta^2)(\zeta^2-8\zeta\eta+\eta^2)\\ + 12\zeta^2\eta^2\ln\left(\frac{\zeta}{\eta}\right)\Bigg)\end{aligned} \tag{20}$$

$$\frac{(\mathbf{L}_\mu\mathbf{L}_\nu|\mathbf{R}_\lambda\mathbf{R}_\sigma)}{(\mathbf{L}_\mu|\mathbf{L}_\nu)(\mathbf{R}_\lambda|\mathbf{R}_\sigma)} = \frac{\alpha\zeta}{5}. \tag{21}$$

2.4.2. Infinite/finite domains

Unfortunately, we have not been able to obtain analytic and numerically satisfactory expressions for (**LL**|**EE**) integrals and others of this type. Fortunately, there are comparatively few of these integrals and if we define $a = (A_{p+1} - A_p)/2$, $R = (A_p + a) - A_1$, $\zeta = \mu^2 + \nu^2$ and $m = \lambda + \sigma$ and reformulate the desired ERIs in terms of the potential of the **LL** product, we obtain

$$\begin{aligned}\frac{(\mathbf{L}_\mu\mathbf{L}_\nu|\mathbf{E}_\lambda^p\mathbf{E}_\sigma^p)}{(\mathbf{L}_\mu|\mathbf{L}_\nu)(\mathbf{E}_\lambda^p|\mathbf{E}_\sigma^p)} = &\frac{\zeta^3}{a^{2m+1}\sqrt{\pi}}\frac{\Gamma(m+3/2)}{\Gamma(m+1)}\\ &\times\int_{R-a}^{R+a}(a^2+(R-x)^2)^m x^2\\ &\times U(3,3,\zeta x)\,dx\end{aligned} \tag{22}$$

$$\begin{aligned}\frac{(\mathbf{L}_\mu\mathbf{L}_\nu|\mathbf{E}_\lambda^p\mathbf{O}_\sigma^p)}{(\mathbf{L}_\mu|\mathbf{L}_\nu)(\mathbf{O}_\lambda^p|\mathbf{O}_\sigma^p)} = -&\frac{2\zeta^3}{a^{2m+2}\sqrt{\pi}\sqrt{3+4\lambda}}\frac{\Gamma(m+5/2)}{\Gamma(m+1)}\\ &\times\int_{R-a}^{R+a}(a^2+(R-x)^2)^m\\ &\times(R-x)x^2U(3,3,\zeta x)\,dx\end{aligned} \tag{23}$$

$$\frac{(\mathbf{L}_\mu\mathbf{L}_\nu|\mathbf{O}^p_\lambda\mathbf{O}^p_\sigma)}{(\mathbf{L}_\mu|\mathbf{L}_\nu)(\mathbf{O}^p_\lambda|\mathbf{O}^p_\sigma)} = \frac{2\zeta^3}{a^{2m+3}\sqrt{\pi}}\frac{\Gamma(m+5/2)}{\Gamma(m+1)} \times \int_{R-a}^{R+a}(a^2+(R-x)^2)^m \times (R-x)^2x^2U(3,3,\zeta x)\,dx. \quad (24)$$

We have found that these can be evaluated satisfactorily by numerical quadrature. The (**RR**|**EE**) integrals and others can be found in the same way.

It is possible to obtain the $(\mathbf{L}_\mu\mathbf{L}_\nu|\mathbf{O}^p_\lambda\mathbf{O}^p_\sigma)$ integral by using the relation

$$\frac{(\mathbf{O}^p_\mu\mathbf{O}^p_\nu|}{(\mathbf{O}^p_\mu|\mathbf{O}^p_\nu)} = (3+2(\mu+\nu))\frac{(\mathbf{E}^p_\mu\mathbf{E}^p_\nu|}{(\mathbf{E}^p_\mu|\mathbf{E}^p_\nu)} - (2+2(\mu+\nu))\frac{(\mathbf{E}^p_\mu\mathbf{E}^p_{\nu+1}|}{(\mathbf{E}^p_\mu|\mathbf{E}^p_{\nu+1})} \quad (25)$$

but we do not currently make use of this.

2.4.3. *Finite/finite domains*

The final class of two-domain ERIs are those between two finite domains. We have constructed a four-term recurrence relation for the calculation of these integrals. Let $f^p = f(x-P)$ be a polynomial basis function pair in the domain p and centred around the point P. Let $g^q = g(y-Q)$ be another function pair in the domain q centred around the point Q. Then we have the following

$$\begin{aligned}(f^p|g^q) &= \int_{-\infty}^{\infty}\int_{-\infty}^{\infty}\frac{f(x-P)g(y-Q)}{y-x}dxdy \\ &= \int_{-\infty}^{\infty}\int_{-\infty}^{\infty}f(x-P)\left(\int_0^\infty e^{-s(y-x)}ds\right) \times g(y-Q)dxdy \\ &= \int_0^\infty\left(\int_{-\infty}^{\infty}f(x-P)e^{sx}dx\right) \times \left(\int_{-\infty}^{\infty}g(y-Q)e^{-sy}dy\right)ds \\ &= \int_0^\infty \mathcal{L}_f(-s)\mathcal{L}_g(s)e^{-(Q-P)s}ds, \end{aligned} \quad (26)$$

where $\mathcal{L}_f$ and $\mathcal{L}_g$ are the Laplace transforms of the basis functions pairs f^p and g^q translated so that they are centred around 0 respectively. Let $a = (A_{p+1} - A_p)/2$ be half the width of the domain p. The required Laplace transforms are

$$\frac{\mathcal{L}[\mathbf{E}^p_\mu\mathbf{E}^p_\nu](s)}{(\mathbf{E}^p_\mu|\mathbf{E}^p_\nu)} = {}_0F_1\left(\mu+\nu+\frac{3}{2};\left(\frac{as}{2}\right)^2\right) \quad (27)$$

$$\frac{\mathcal{L}[\mathbf{E}^p_\mu\mathbf{O}^p_\nu](s)}{(\mathbf{O}^p_\mu|\mathbf{O}^p_\nu)} = -\frac{as}{\sqrt{4\mu+3}}{}_0F_1\left(\mu+\nu+\frac{3}{2};\left(\frac{as}{2}\right)^2\right), \quad (28)$$

where ${}_0F_1(c;x)$ is the confluent hypergeometric limit function, which obeys the following three-term recurrence relation [44]

$${}_0F_1(c-1;x) - {}_0F_1(c;x) = \frac{x}{c(c-1)}{}_0F_1(c+1;x). \quad (29)$$

Since we are interested in products of the functions in Equations (27) and (28), both of which contain the same argument to the hypergeometric function, we are able to apply the recurrence relation (29) twice and remove the additional argument dependence. Let $m = \mu + \nu$, $n = \lambda + \sigma$, $a = (A_{p+1} - A_p)/2$ and $b = (A_{q+1} - A_q)/2$, then

$$\begin{aligned}&{}_0F_1\left(m-\frac{1}{2};\frac{a^2s^2}{4}\right){}_0F_1\left(n+\frac{3}{2};\frac{b^2s^2}{4}\right) \\ &= {}_0F_1\left(m+\frac{1}{2};\frac{a^2s^2}{4}\right){}_0F_1\left(n+\frac{3}{2};\frac{b^2s^2}{4}\right) \\ &\quad + \frac{a^2(n-\frac{1}{2})(n+\frac{1}{2})}{b^2(m-\frac{1}{2})(m+\frac{1}{2})}{}_0F_1\left(m+\frac{3}{2};\frac{a^2s^2}{4}\right) \\ &\quad \times\left[{}_0F_1\left(n-\frac{1}{2};\frac{b^2s^2}{4}\right) - {}_0F_1\left(n+\frac{1}{2};\frac{b^2s^2}{4}\right)\right]. \end{aligned} \quad (30)$$

This recurrence relation can be applied to the integrals constructed from Equations (26), (27) and (28). As an illustrative example one possible recurrence relation is

$$\begin{aligned}&\frac{(\mathbf{E}^p_{\mu-1}\mathbf{E}^p_\nu|\mathbf{E}^q_\lambda\mathbf{E}^q_\sigma)}{(\mathbf{E}^p_{\mu-1}|\mathbf{E}^p_\nu)(\mathbf{E}^q_\lambda|\mathbf{E}^q_\sigma)} \\ &= \frac{(\mathbf{E}^p_\mu\mathbf{E}^p_\nu|\mathbf{E}^q_\lambda\mathbf{E}^q_\sigma)}{(\mathbf{E}^p_\mu|\mathbf{E}^p_\nu)(\mathbf{E}^q_\lambda|\mathbf{E}^q_\sigma)} + \frac{a^2(n-\frac{1}{2})(n+\frac{1}{2})}{b^2(m+\frac{1}{2})(m+\frac{3}{2})} \\ &\quad \times\left(\frac{(\mathbf{E}^p_{\mu+1}\mathbf{E}^p_\nu|\mathbf{E}^q_{\lambda-2}\mathbf{E}^q_\sigma)}{(\mathbf{E}^p_{\mu+1}|\mathbf{E}^p_\nu)(\mathbf{E}^q_{\lambda-2}|\mathbf{E}^q_\sigma)} - \frac{(\mathbf{E}^p_{\mu+1}\mathbf{E}^p_\nu|\mathbf{E}^q_{\lambda-1}\mathbf{E}^q_\sigma)}{(\mathbf{E}^p_{\mu+1}|\mathbf{E}^p_\nu)(\mathbf{E}^q_{\lambda-1}|\mathbf{E}^q_\sigma)}\right). \end{aligned} \quad (31)$$

Numerical experiments suggest that this backwards recurrence in μ is sufficiently stable for our purposes but that the forward recurrence is unstable. This necessitates the construction of starting values for the recurrence. Two sets of starting values are required, and these sets can be viewed as two rows where $m = \mu + \nu$ is small and two columns where $n = \lambda + \sigma$ is large. Figure 2 shows a graphical representation of the recurrence.

Obtaining the two columns where n is large can be achieved adequately by using the power series definition of the ${}_0F_1$ hypergeometric function

$${}_0F_1(a;z) = \sum_{k=1}^{\infty}\frac{1}{(a)_k}\frac{z^k}{k!} \quad (32)$$

$$(a)_k = a(a+1)(a+2)\ldots(a+k-1)(a+k), \quad (33)$$

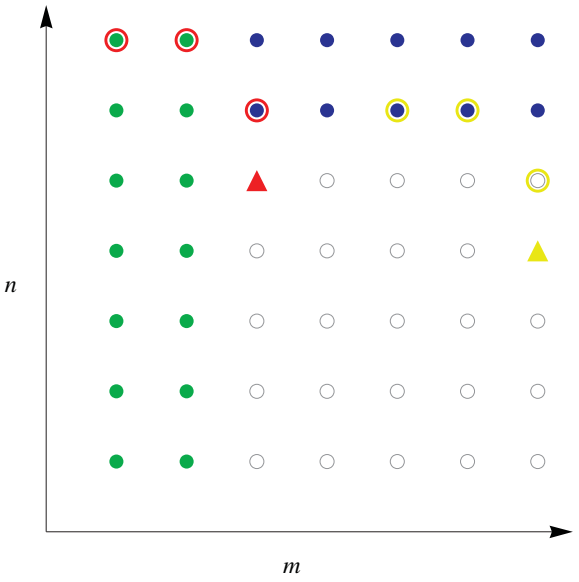

Figure 2 Graphical representation of the recurrence relation for computing electron repulsion integrals between two finite domains. Green dots represent integrals with one small parameter that can be computed by analytic expressions. Blue dots represent integrals that are evaluated from power series expansions. Grey circles are the integrals to be evaluated by recursion. The red and yellow circles denote the integrals that can be used to form the integrals shown by the red and yellow triangles, respectively.

where $(a)_k$ is the Pochhammer symbol [44]. The terms in the sum decay rapidly when the hypergeometric parameter is of modest size and, as a result, the sum can be truncated after a few terms.

To construct the two rows with small values of $m = \mu + \nu$, we have obtained analytic expressions for the necessary integrals when $m = 0$ and $m = -1$. Let $m = \mu + \nu$, $n = \lambda + \sigma$, $a = (A_{p+1} - A_p)/2$, $b = (A_{q+1} - A_q)/2$ and $R = |(A_q + b) - (A_p + a)|$ be the distance between the centroids of the two domains p and q. Then for two pairs of even polynomials these expressions are

$$\frac{(\mathbf{E}^p_\mu \mathbf{E}^p_\nu|\mathbf{E}^q_\lambda \mathbf{E}^q_\sigma)}{(\mathbf{E}^p_\mu|\mathbf{E}^p_\nu)(\mathbf{E}^q_\lambda|\mathbf{E}^q_\sigma)} = \frac{1}{2}\left[\frac{1}{R-a}\,{}_2F_1\left(\frac{1}{2},1;n+\frac{3}{2};\frac{b^2}{(R-a)^2}\right) + \frac{1}{R+a}\,{}_2F_1\left(\frac{1}{2},1;n+\frac{3}{2};\frac{b^2}{(R+a)^2}\right)\right] \qquad m=-1 \tag{34}$$

$$\frac{(\mathbf{E}^p_\mu \mathbf{E}^p_\nu|\mathbf{E}^q_\lambda \mathbf{E}^q_\sigma)}{(\mathbf{E}^p_\mu|\mathbf{E}^p_\nu)(\mathbf{E}^q_\lambda|\mathbf{E}^q_\sigma)} = \frac{1}{8a}\left[\frac{2b^2}{(3+2n)(R-a)^2} \times {}_3F_2\left(1,1,\frac{3}{2};2,n+\frac{5}{2};\frac{b^2}{(R-a)^2}\right) - \frac{2b^2}{(3+2n)(R+a)^2} \times {}_3F_2\left(1,1,\frac{3}{2};2,n+\frac{5}{2};\frac{b^2}{(R+a)^2}\right) - 4\left(\ln(R-a)-\ln(R+a)\right)\right] \qquad m=0. \tag{35}$$

For a pair of even functions interacting with a pairing of an even and an odd polynomial, the expressions are

$$\begin{aligned}\frac{(\mathbf{E}^p_\mu \mathbf{E}^p_\nu|\mathbf{E}^q_\lambda \mathbf{O}^q_\sigma)}{(\mathbf{E}^p_\mu|\mathbf{E}^p_\nu)(\mathbf{O}^q_\lambda|\mathbf{O}^q_\sigma)} &= -\frac{b}{2\sqrt{3+4\lambda}}\left[\frac{(3+2n)[(3+2n)(R-a)^2-b^2]}{((R-a)^2-b^2)^2} - \frac{4(1+n)(2+n)(R-a)^2}{((R-a)^2-b^2)^2} \times {}_2F_1\left(-\frac{1}{2},1;n+\frac{5}{2};\frac{b^2}{(R-a)^2}\right) + \frac{(3+2n)[(3+2n)(R+a)^2-b^2]}{((R+a)^2-b^2)^2} - \frac{4(1+n)(2+n)(R+a)^2}{((R+a)^2-b^2)^2} \times {}_2F_1\left(-\frac{1}{2},1;n+\frac{5}{2};\frac{b^2}{(R+a)^2}\right)\right] \\ &\qquad m=-1\end{aligned} \tag{36}$$

$$\frac{(\mathbf{E}^p_\mu \mathbf{E}^p_\nu|\mathbf{E}^q_\lambda \mathbf{O}^q_\sigma)}{(\mathbf{E}^p_\mu|\mathbf{E}^p_\nu)(\mathbf{O}^q_\lambda|\mathbf{O}^q_\sigma)} = -\frac{b}{2a\sqrt{3+4\lambda}}\left[\frac{1}{R-a}\,{}_2F_1\left(\frac{1}{2},1;n+\frac{5}{2};\frac{b^2}{(R-a)^2}\right) + \frac{1}{R+a}\,{}_2F_1\left(\frac{1}{2},1;n+\frac{5}{2};\frac{b^2}{(R+a)^2}\right)\right] \qquad m=0. \tag{37}$$

Note that when the two domains being integrated over are adjacent, it is necessary to take the limit as $R - a \to 0$.

It is not necessary to consider any more integrals. Using Equation (25) both bras and kets containing pairs of odd basis functions can be constructed from those over pairs of even functions. Additionally, integrals over two mixed pairs (one even and one odd function) can be formed from the integral over two pairs of even functions

$$\frac{(\mathbf{E}^p_\mu \mathbf{O}^p_\nu|\mathbf{E}^q_\lambda \mathbf{O}^q_\sigma)}{(\mathbf{O}^p_\mu|\mathbf{O}^p_\nu)(\mathbf{O}^q_\lambda|\mathbf{O}^q_\sigma)} = -\frac{4b}{a}\frac{(m+1/2)(m+3/2)}{\sqrt{3+4\mu}\sqrt{3+4\lambda}} \times \left(\frac{(\mathbf{E}^p_{\mu-1}\mathbf{E}^p_\nu|\mathbf{E}^q_{\lambda+1}\mathbf{E}^q_\sigma)}{(\mathbf{E}^p_{\mu-1}|\mathbf{E}^p_\nu)(\mathbf{E}^q_{\lambda+1}|\mathbf{E}^q_\sigma)} - \frac{(\mathbf{E}^p_\mu \mathbf{E}^p_\nu|\mathbf{E}^q_{\lambda+1}\mathbf{E}^q_\sigma)}{(\mathbf{E}^p_\mu|\mathbf{E}^p_\nu)(\mathbf{E}^q_{\lambda+1}|\mathbf{E}^q_\sigma)}\right). \tag{38}$$

Any other required integrals can be obtained via symmetry.

2.5. One-domain two-electron integrals

We now turn our attention to integrals where all four basis functions reside in the same domain. Here, one find that the Coulomb and exchange components of the antisymmetrised integral diverge but their sum is finite. To treat these, we rewrite the Coulomb operator as the limit of a sequence of softened potentials $\mathrm{erf}\,(\omega(x-y))/(x-y)$, where ω determines the degree of softening.

Taking the Fourier transform of this operator allows us to also bring the two basis function pairs into frequency space. Let $(\mathbf{F}^p_\mu\mathbf{F}^p_\nu|\mathbf{F}^p_\lambda\mathbf{F}^p_\sigma)_\omega$ denote a two-electron integral using the softened Coulomb operator, $\mathcal{F}_{\mu\nu} = \mathcal{F}[\mathbf{F}^p_\mu\mathbf{F}^p_\nu]$ be the Fourier transform of the product $\mathbf{F}^p_\mu\mathbf{F}^p_\nu$, $\Gamma(a,x)$ denote the incomplete gamma function and γ denote Euler's constant, then we find

$$\begin{aligned}
\left(\mathbf{F}^p_\mu\mathbf{F}^p_\nu|\mathbf{F}^p_\lambda\mathbf{F}^p_\sigma\right)_\omega &= \left(\mathbf{F}^p_\mu\mathbf{F}^p_\nu\left|\frac{\mathrm{erf}\,(\omega(x-y))}{x-y}\right|\mathbf{F}^p_\lambda\mathbf{F}^p_\sigma\right)\\
&= \left(\mathbf{F}^p_\mu\mathbf{F}^p_\nu\left|\frac{1}{2\pi}\int_{-\infty}^{\infty}\Gamma\left(0,\frac{k^2}{4\omega^2}\right)\right.\right.\\
&\quad\left.\left.\times e^{ik(x-y)}dk\right|\mathbf{F}^p_\lambda\mathbf{F}^p_\sigma\right)\\
&= \frac{1}{2\pi}\int_{-\infty}^{\infty}\Gamma\left(0,\frac{k^2}{4\omega^2}\right)\left(\int_{A_p}^{A_{p+1}}\mathbf{F}^p_\mu\mathbf{F}^p_\nu e^{ikx}dx\right)\\
&\quad\times\left(\int_d\mathbf{F}^p_\lambda\mathbf{F}^p_\sigma e^{-iky}dy\right)dk\\
&= \frac{1}{2\pi}\int_{-\infty}^{\infty}\Gamma\left(0,\frac{k^2}{4\omega^2}\right)\mathcal{F}_{\mu\nu}(k)\mathcal{F}_{\lambda\sigma}(-k)dk\\
&= \frac{1}{2\pi}\left[\int_{-\infty}^{\infty}\left(2\sinh^{-1}(\sqrt{2}\omega)-\gamma-3\ln 2\right)\right.\\
&\quad\times\mathcal{F}_{\mu\nu}(k)\mathcal{F}_{\lambda\sigma}(-k)\,dk\\
&\quad+\int_{-\infty}^{\infty}\left(\Gamma\left(0,\frac{k^2}{4\omega^2}\right)-2\sinh^{-1}(\sqrt{2}\omega)\right.\\
&\quad\left.\left.+\gamma+3\ln 2\right)\mathcal{F}_{\mu\nu}(k)\mathcal{F}_{\lambda\sigma}(-k)\,dk\right]. \qquad (39)
\end{aligned}$$

$$\begin{aligned}
\left(\mathbf{F}^p_\mu\mathbf{F}^p_\nu||\mathbf{F}^p_\lambda\mathbf{F}^p_\sigma\right) &= \lim_{\omega\to\infty}\left(\mathbf{F}^p_\mu\mathbf{F}^p_\nu|\mathbf{F}^p_\lambda\mathbf{F}^p_\sigma\right)_\omega-\left(\mathbf{F}^p_\mu\mathbf{F}^p_\lambda|\mathbf{F}^p_\nu\mathbf{F}^p_\sigma\right)_\omega\\
&= \lim_{\omega\to\infty}\left[\frac{1}{2\pi}\left(2\sinh^{-1}(\sqrt{2}\omega)-\gamma-3\ln 2\right)\right.\\
&\quad\times\left(\int_{-\infty}^{\infty}\mathcal{F}_{\mu\nu}(k)\mathcal{F}_{\lambda\sigma}(-k)dk\right.\\
&\quad\left.-\int_{-\infty}^{\infty}\mathcal{F}_{\mu\lambda}(k)\mathcal{F}_{\nu\sigma}(-k)dk\right)\\
&\quad+\frac{1}{2\pi}\int_{-\infty}^{\infty}\left(\Gamma\left(0,\frac{k^2}{4\omega^2}\right)\right.\\
&\quad\left.-2\sinh^{-1}(\sqrt{2}\omega)+\gamma+3\ln 2\right)\\
&\quad\times\left(\mathcal{F}_{\mu\nu}(k)\mathcal{F}_{\lambda\sigma}(-k)\right.\\
&\quad\left.\left.-\mathcal{F}_{\mu\lambda}(k)\mathcal{F}_{\nu\sigma}(-k)\right)dk\right]. \qquad (40)
\end{aligned}$$

We can use the following relationship, which is a consequence of Parseval's theorem [44], to remove the first term within the limit

$$\begin{aligned}
\int_{-\infty}^{\infty}\mathcal{F}_{\mu\nu}(k)\mathcal{F}_{\lambda\sigma}(-k)dk &= \int_{A_p}^{A_{p+1}}\mathbf{F}^p_\mu(r)\mathbf{F}^p_\nu(r)\mathbf{F}^p_\lambda(r)\mathbf{F}^p_\sigma(r)dr\\
&= \int_{-\infty}^{\infty}\mathcal{F}_{\mu\lambda}(k)\mathcal{F}_{\nu\sigma}(-k)dk \qquad (41)
\end{aligned}$$

and obtain

$$\begin{aligned}
\left(\mathbf{F}^p_\mu\mathbf{F}^p_\nu||\mathbf{F}^p_\lambda\mathbf{F}^p_\sigma\right) &= \lim_{\omega\to\infty}\left[\frac{1}{2\pi}\int_{-\infty}^{\infty}\left(\Gamma\left(0,\frac{k^2}{4\omega^2}\right)\right.\right.\\
&\quad\left.-2\sinh^{-1}(\sqrt{2}\omega)+\gamma+3\ln 2\right)\\
&\quad\times\left(\mathcal{F}_{\mu\nu}(k)\mathcal{F}_{\lambda\sigma}(-k)\right.\\
&\quad\left.\left.-\mathcal{F}_{\mu\lambda}(k)\mathcal{F}_{\nu\sigma}(-k)\right)dk\right]\\
&= \left\{\mathbf{F}^p_\mu\mathbf{F}^p_\nu|\mathbf{F}^p_\lambda\mathbf{F}^p_\sigma\right\}-\left\{\mathbf{F}^p_\mu\mathbf{F}^p_\lambda|\mathbf{F}^p_\nu\mathbf{F}^p_\sigma\right\} \qquad (42)
\end{aligned}$$

where we have introduced the 'quasi-integral'

$$\left\{\mathbf{F}^p_\mu\mathbf{F}^p_\nu|\mathbf{F}^p_\lambda\mathbf{F}^p_\sigma\right\} = -\frac{1}{2\pi}\int_{-\infty}^{\infty}\mathcal{F}_{\mu\nu}(k)\mathcal{F}_{\lambda\sigma}(-k)\ln\left(\frac{k^2}{4}\right)dk. \qquad (43)$$

There are two cases: (1) the domain is infinite; (2) the domain is finite.

2.5.1. *Infinite/infinite quasi-integrals*

It is easy to show that

$$\begin{aligned}
\frac{\{\mathbf{L}_\mu\mathbf{L}_\nu|\mathbf{L}_\lambda\mathbf{L}_\sigma\}}{(\mathbf{L}_\mu|\mathbf{L}_\nu)(\mathbf{L}_\lambda|\mathbf{L}_\sigma)} &= \frac{\{\mathbf{R}_\mu\mathbf{R}_\nu|\mathbf{R}_\lambda\mathbf{R}_\sigma\}}{(\mathbf{R}_\mu|\mathbf{R}_\nu)(\mathbf{R}_\lambda|\mathbf{R}_\sigma)}\\
&= \alpha\zeta\eta\left(\frac{\zeta^2+6\zeta\eta+\eta^2}{2(\zeta+\eta)^3}-\frac{6\zeta^2\eta^2\ln\zeta\eta}{(\zeta+\eta)^5}\right). \qquad (44)
\end{aligned}$$

2.5.2. *Finite/finite quasi-integrals*

Because of symmetry, only the $\{\mathbf{E}^p_\mu\mathbf{E}^p_\nu|\mathbf{E}^p_\lambda\mathbf{E}^p_\sigma\}$, $\{\mathbf{E}^p_\mu\mathbf{E}^p_\mu|\mathbf{O}^p_\lambda\mathbf{O}^p_\sigma\}$, $\{\mathbf{O}^p_\mu\mathbf{O}^p_\nu|\mathbf{O}^p_\lambda\mathbf{O}^p_\sigma\}$ and $\{\mathbf{E}^p_\mu\mathbf{O}^p_\nu|\mathbf{E}^p_\lambda\mathbf{O}^p_\sigma\}$ integral classes are non-vanishing and, if the relationship (25) is exploited, it is necessary only to compute the first and last of these classes.

We have been unable to find a general expression for these quasi-integrals. However, because they scale inversely

with the width of the domain, we have tabulated the necessary quasi-integrals for a domain on the interval $[-1, 1]$ and our program simply scales these, as required, on the fly.

3. Implementation

We have implemented the above theory in a new program that we call CHEM1D. So that others may understand how the results of Section 2 are used practically, we present an overview of the structure of CHEM1D. In the following section, we define $\mathcal{D}$ to be the set of all domains (both finite and infinite) in the molecule, $\mathcal{D}_I$ and $\mathcal{D}_F$ to be the set of all infinite and finite domains, respectively, $N(p)$ to be the total number of basis functions in the domain p and $E(p)$ and $O(p)$ to be the number of even and odd basis functions, respectively, in the finite domain p.

3.1. Integral evaluation

The heart of any quantum chemistry program is its integral evaluation routines, particularly those for the two-electron integrals, for it is these quantities that typically represent the computational bottleneck and make the heaviest demand on computer memory. Our algorithms are not optimal but we have attempted to exploit some of the simplifications that arise as a consequence of the domain separation of electrons.

3.1.1. One-electron integrals

Because the product of two basis functions in different domains vanishes, the one-electron integral matrices are block diagonal with each block corresponding to a domain. Therefore, for each of the three matrices, and for each domain $p \in \mathcal{D}$, we create a square matrix of size $N(p)$.

Because the integrals can be computed from analytic expressions, computing the content of these matrices is a relatively simple process. We use three subroutines: one for the overlap, one for the kinetic energy and one for the nuclear-attraction energy. Each routine operates over one domain with each call.

Let S^p, T^p and V^p be the overlap, kinetic and nuclear-attraction matrix for the domain p, respectively, and Z_n be the charge of the nth nucleus. Pseudocode describing our methods for computing these integrals can be seen in Algorithm 1.

3.1.2. Two-domain two-electron integrals

We now turn our attention to the significantly more complicated two-electron integrals. As described in Section 2.4, these integrals can be separated into two classes. We begin with the case of non-overlapping integrals, which can be further separated into another three subclasses: integrals

Algorithm 1. One-electron integrals

procedure OVERLAP(p) ▷ Computes S^p
  if p is an infinite domain **then**
    for $i, j = 1 \to N(p)$ **do**
      $S^p_{i,j}$ = Equation (6)
    end for
  else
    for $i, j = 1 \to E(p)$ **do**
      $S^p_{i,j}$ = Equation (7)
      ▷ Compute Γ ratios by recursion
    end for
    for $i, j = 1 \to O(p)$ **do**
      $S^p_{i+E(p),j+E(p)}$ = Equation (8)
    end for
  end if
end procedure
procedure KINETIC(p) ▷ Computes T^p
  if p is an infinite domain **then**
    for $i, j = 1 \to N(p)$ **do**
      $T^p_{i,j} = S^p_{i,j} \times$ Equation (9)
    end for
  else
    for $i, j = 1 \to E(p)$ **do**
      $T^p_{i,j} = S^p_{i,j} \times$ Equation (10)
    end for
    for $i, j = 1 \to O(p)$ **do**
      $T^p_{i+E(p),j+E(p)} = S^p_{i+E(p),j+E(p)} \times$ Equation (11)
    end for
  end if
end procedure
procedure POTENTIAL(p) ▷ Computes V^p
  if p is an infinite domain **then**
    for $i, j = 1 \to N(p)$ **do**
      $V^p_{i,j}$ = Equations (12) or (13)
    end for
  else
    for $i, j = 1 \to E(p)$ **do**
      $V^p_{i,j}$ = Equation (14)
    end for
    for $i = 1 \to E(p), j = 1 \to O(p)$ **do**
      $V^p_{i,j+E(p)}$ = Equation (16)
      $V^p_{j+E(p),i} = V^p_{i,j+E(p)}$
    end for
    for $i, j = 1 \to O(p)$ **do**
      $V^p_{i+E(p),j+E(p)}$ = Equation (15)
    end for
  end if
end procedure

between two infinite domains, integrals between a finite and an infinite domain and integrals between two finite domains.

For convenience, we store the full set of ERIs and this is feasible for all of the molecules reported here. The integrals are stored in a four-index array for each pair of domains (p, q) in the molecule. The first two indices of each array are of length $N(p)$, while the last two indices are of length $N(q)$.

When both domains are infinite, we use the analytic expressions in Equations (18)–(21). When the system is not an atom, this requires the evaluation of a confluent hypergeometric function. We evaluate these functions before entering the loop structure for the integrals; the hypergeometric function is required twice for most evaluations, one call dependent on the two basis functions from p and one on the two basis functions from q. An overview of the procedure we use here can be found in Algorithm 2.

Algorithm 2. Two-electron integrals between infinite domains

procedure INF-INF(p, q)
  if the system is an atom **then**
    for $\mu, \nu = 1, N(p)$ **do**
      $\zeta = \mu^2 + \nu^2$
      for $\lambda, \sigma = 1, N(q)$ **do**
        $\eta = \lambda^2 + \sigma^2$
        if $\zeta = \eta$ **then**
          $(\mu\nu|\lambda\sigma) = S^p_{\mu\nu}\, S^q_{\lambda\sigma} \times$ Equation (21)
        else
          $(\mu\nu|\lambda\sigma) = S^p_{\mu\nu}\, S^q_{\lambda\sigma} \times$ Equation (20)
        end if
      end for
    end for
  else
    for $\mu, \nu = 1, \max(N(p), N(p))$ **do**
      Precompute $U\left(1, 1, R\alpha(\mu^2 + \nu^2)\right)$
    end for
    for $\mu, \nu = 1, N(p)$ **do**
      $\zeta = \mu^2 + \nu^2$
      for $\lambda, \sigma = 1, N(q)$ **do**
        $\eta = \lambda^2 + \sigma^2$
        if $\zeta = \eta$ **then**
          $(\mu\nu|\lambda\sigma) = S^p_{\mu\nu}\, S^q_{\lambda\sigma} \times$ Equation (19)
        else
          $(\mu\nu|\lambda\sigma) = S^p_{\mu\nu}\, S^q_{\lambda\sigma} \times$ Equation (18)
        end if
      end for
    end for
  end if
end procedure

When p is an infinite domain and q is a finite domain (or vice versa), we use a 500-point trapezoidal rule to achieve the quadrature described above. This is simple to implement and affords sufficient accuracy. The most expensive step in the quadrature is the evaluation of confluent hypergeometric functions. These can be evaluated within the loop structure for selecting a basis set pair in the infinite domain, but before the loop structure for the finite domain. They can then be kept in temporary storage and used for all three types of finite domain basis function pairs. Pseudocode for the evaluation of this class can be found in Algorithm 3; we assume p to be the infinite domain.

Algorithm 3. Two-electron integrals between infinite and finite domains

procedure INF_FIN(p, q)
  for $\mu, \nu = 1, N(p)$ **do**
    $\zeta = \mu^2 + \nu^2$
    for $i = 1, 500$ **do**
      Compute $U(3, 3, \zeta x_i)$
    end for
    for $\lambda, \sigma = 1, E(q)$ **do**
      $(\mu\nu|\lambda\sigma) = S^p_{\mu\nu}\, S^q_{\lambda\sigma} \times$ Equation (22)
        ▷ Computed using trapezoidal rule
    end for
    for $\lambda = 1, E(q), \sigma = 1, O(q)$ **do**
      $(\mu\nu|\lambda\sigma) = S^p_{\mu\nu}\, S^q_{\lambda\sigma} \times$ Equation (23)
        ▷ Computed using trapezoidal rule
      $(\mu\nu|\sigma\lambda) = (\mu\nu|\lambda\sigma)$
    end for
    for $\lambda, \sigma = 1, O(q)$ **do**
      $(\mu\nu|\lambda\sigma) = S^p_{\mu\nu}\, S^q_{\lambda\sigma} \times$ Equation (24)
        ▷ Computed using trapezoidal rule
    end for
  end for
end procedure

The final classes of two-domain integrals are those involving finite domains. This step requires the most complex code in CHEM1D due to the need to calculate starting values for the various recurrences from a variety of methods, execute the recurrences and correctly pack the resulting prototype integrals into the appropriate parts of the storage arrays. To handle these steps, we use three levels of routines. The bottom level computes the necessary starting values for the recurrence relations used. The middle level computes the prototype integrals using the recurrence relations described in Section 2.4.3. The top level then transfers the completed prototype integrals from temporary storage into the final storage arrays.

The middle subroutines are straightforward implementations of our four-term recurrence relation. During the top level procedure, we make extensive use of the symmetry allowed by the use of real-valued basis functions, which minimises the looping structures required to traverse the many possible arrangements of integrals. This requires a great deal of care to ensure that the integrals are scattered into the correct storage spaces, but is ultimately a straightforward process.

The most complicated routines for computing recurrence starting values are those for when $\mu + \nu = -1$, 0. The analytic expressions that must be evaluated contain two different hypergeometric functions. To evaluate these we employ backward recurrence, using the power series expansion to evaluate the starting points. For illustrative purposes, we give an outline of the code for the computation of integrals of the types $(\mathbf{E}^p_\mu \mathbf{E}^p_\nu | \mathbf{E}^q_\lambda \mathbf{E}^q_\sigma)$ and $(\mathbf{E}^p_\mu \mathbf{E}^p_\nu | \mathbf{O}^q_\lambda \mathbf{O}^q_\sigma)$ in Algorithm 4.

3.1.3. *Quasi-integrals*

Constructing the quasi-integrals for the single-domain case is significantly simpler than building the integrals for the two-domain cases. For the infinite domains, we use the analytic expression in Equation (44), which requires no special functions. As stated above, we scale a set of standard integrals for the finite domain. We have used Mathematica [45] to compute the analytic solution to the integrals for a domain on the line segment $[-1, 1]$ and evaluate them to high precision. These values are appropriately scaled by CHEM1D as needed.

We use two subroutines to perform these tasks: QUASI_INF(p) gives the integrals for the infinite domain p and QUASI_FIN(q) those for the finite domain q.

3.1.4. *Antisymmetrised integrals*

The above routines are all called by a driver routine which handles the looping over the domain structures. In our implementation, this routine is also responsible for managing the temporary storage space required and locating the appropriate areas of memory for storing the single-bar and quasi-integrals for each pairing of p and q. The contraction of quasi-integrals to form correct double-bar integrals in the case of overlapping domains is handled by a separate subroutine. This operation is almost identical to that required for normal three-dimensional (3D) quantum chemical calculations; as such we have excluded its pseudocode. The driver routine however is described in Algorithm 5.

3.2. *Self-consistent field calculations*

Once the necessary integrals have been evaluated, CHEM1D uses them to compute the Hartree–Fock self-consistent field (SCF) energy followed by the second- and third-order Møller–Plesset perturbation energies. The formulations used are those described in the text by Szabo and Ostlund [43]; some modifications to the Hartree–Fock methods are made however, mostly to exploit the domain separation of the electrons.

Like most basis sets used in quantum chemistry, the basis sets described in Section 2.2 are not orthogonal. In order to perform the iterative SCF procedure for computing the Hartree–Fock energy, it is necessary to transform

Algorithm 4. Two-electron integrals between finite domains

procedure FIN_FIN(p, q)
  MaxM $= 2\max(E(p), E(q), O(p), O(q)) + 1$
  Allocate proto(-1 : MaxM, -1 : MaxM)
    ▷ Used to store prototype integrals
  EEEE_PROTOTYPES(MaxM, proto)
  for $\mu, \nu = 1, E(p)$ **do**
    for $\lambda, \sigma = 1, E(q)$ **do**
      $(\mu\nu|\lambda\sigma) = S^p_{\mu\nu}\, S^q_{\lambda\sigma} \times \text{proto}(\mu + \nu, \lambda + \sigma)$
      $(\lambda\sigma|\mu\nu) = (\mu\nu|\lambda\sigma)$
    end for
    for $\lambda, \sigma = 1, O(q)$ **do**
      $(\mu\nu|\lambda\sigma) = S^p_{\mu\nu}\, S^q_{\lambda\sigma} \times [(3 + 2(\lambda + \sigma))$
      $\text{proto}(\mu + \nu, \lambda + \sigma) - (2 + 2(\lambda + \sigma))$
      $\times \text{proto}(\mu + \nu, \lambda + \sigma + 1)]$
      ▷ Using Equation (25)
      $(\lambda\sigma|\mu\nu) = (\mu\nu|\lambda\sigma)$
    end for
  end for
  ⋮
end procedure
procedure EEEE_PROTOTYPES(MaxM, proto)
  M_MINUS_ONE(proto(:, -1))
  M_ZERO(proto(:, 0))
  for $i = 1$, MaxM **do**
    proto(MaxM, i) = (34)
    proto(MaxM $-$ 1, i) = (35)
      ▷ Compute from power series
  end for
  for $n = 1$, MaxM **do**
    for $m =$ MaxM $- 2, 1, -1$ **do**
      Generate proto(m, n) using Equation (31)
        ▷ $m = \mu + \nu, n = \lambda + \sigma$
    end for
  end for
end procedure
procedure M_MINUS_ONE(*output*)
  Compute hypergeometrics in (34) for $\mu + \nu =$ MaxM, MaxM $- 1$
    ▷ From power series
  for $m =$ MaxM $- 2, 1, -1$ **do**
    Compute hypergeometrics in (34) for $\mu + \nu = m$ via recurrence
  end for
  Combine hypergeometric functions and store in *output*
    ▷ Using Equation (34)
end procedure
procedure M_ZERO(output)
  Compute hypergeometrics in (35) for $\mu + \nu =$ MaxM, MaxM $- 1$
    ▷ From power series
  for $m =$ MaxM $- 2, 1, -1$ **do**
    Compute hypergeometrics in (35) for $\mu + \nu = m$ via recurrence
  end for
  Combine hypergeometric functions and store in *output*
    ▷ Using Equation (35)
end procedure

Algorithm 5. Electron repulsion integral driver

```
1: procedure ERI
2:     INF_INF
3:     for p ∈ D_I do
4:         QUASI_INF(p)
5:         for q ∈ D_F do
6:             INF_FIN(p, q)
7:         end for
8:     end for
9:     for p ∈ D_F do
10:        QUASI_FIN(p)
11:        for q ∈ D_F do
12:            FIN_FIN(p, q)
13:        end for
14:    end for
15: end procedure
```

the non-orthogonal basis to an orthogonal one. CHEM1D follows the procedure described by Szabo and Ostlund [43] for canonical orthogonalisation. We prefer this over symmetric orthogonalisation for numerical reasons. Constructing either of these orthogonalisations requires finding the eigen decomposition for the overlap matrix. This matrix becomes poorly conditioned relatively quickly due to the basis sets we use. The canonical orthogonalisation allows us to account for this by removing columns of the matrix; the symmetric orthogonalisation does not, resulting in a large loss of precision and erratic SCF behaviour. Note that since this matrix is dependent upon the overlap matrix it inherits the same block structure.

Three quantities remain to be considered before an SCF iteration can be described. The first two of these are the density and orbital coefficient matrices. An initial guess at the orbitals is needed; CHEM1D currently uses the zero matrix as a guess and we have found this to be sufficient for most purposes. It is then possible to generate the density matrix from the orbital coefficients as described by Szabo and Ostlund [43].

Each orbital must be constructed of basis functions in only one domain; however, constructing an orbital from basis functions in multiple domains implies that an electron occupying it would be able to move across nuclei, violating impenetrability. Both the density matrix and the orbital coefficient matrix therefore have the same block structure as the one-electron matrices. We can store both of these and construct the density matrix domain by domain.

The final matrix that is needed to perform an SCF cycle is referred to as the G matrix by Szabo and Ostlund. This matrix measures the average repulsion of an electron in the field of all others and is given by the following formula:

$$G_{\mu,\nu} = \sum_{\lambda\sigma} P_{\lambda,\sigma}(\mu\nu||\lambda\sigma), \tag{45}$$

where P is the density matrix. The reliance on P forces λ and σ to be in the same domain; the sum can then be separated further into another sum over each domain. For the integral $(\mu\nu||\lambda\sigma)$ to be non-zero, μ and ν must then also be in the same domain, giving the matrix G the same block structure as all the previous matrices we have considered. We give our algorithm for the construction of G over a given domain p in Algorithm 6.

Algorithm 6. Construction of the two-electron G^p matrix

```
1: procedure BUILD_G(p)
2:     for q ∈ D do   ▷ Find the interaction of domain p
3:                        with every other domain
4:         for μ, ν = 1, N(p) do
5:             G^p_{μ,ν} = Σ_{λ,σ=1}^{N(q)} P^q_{λσ}(μν||λσ)
6:                    ▷ P^q is the density in domain q
7:         end for
8:     end for
9: end procedure
```

We have now described the necessary components for an SCF iteration to be evaluated. However, thanks to the domain separation present in all the matrices, a significant optimisation can be included: each iteration can be computed over each domain individually. The only exception to this complete separation of the SCF procedure is that the new density in each cycle must be calculated for each domain before the cycle can begin; this ensures the correct coupling between electrons in different domains. We note that this leads to a simple method for parallelisation of the calculation, with the limit that each thread will require race conditions to ensure the iteration over each domain proceeds in lockstep.

We also employ the direct inversion in the iterative subspace (DIIS) method of Pulay [46,47] to accelerate the SCF convergence. It reduces both the build-up of roundoff error and the execution time. By default, the SCF iteration terminates when the root-mean-square of the DIIS error matrix drops below 10^{-6}. We present pseudocode for the procedure we use to evaluate an SCF cycle in Algorithm 7.

3.3. *Møller–Plesset perturbation theory*

The final component of CHEM1D are the routines for calculating Møller–Plesset perturbation corrections to the Hartree–Fock energy. Both the second- and third-order corrections are currently implemented according to the procedure described by Szabo and Ostlund [43]. Our current implementation does not exploit the domain separation and, because of this, these correlation corrections are the slowest parts of the program. Due to the standard nature of our algorithm for these calculations, we have omitted a pseudocode description.

Algorithm 7. SCF iteration

```
1:  procedure SCF_CYCLE
2:      for p ∈ 𝒟 do
3:          BUILD_P(p)
4:                  ▷ Update density matrix for all domains
5:      end for
6:      for p ∈ 𝒟 do
7:          BUILD_G(p)
8:          F_1^p = G^p + T^p + V^p
9:                          ▷ F_1^p is the current Fock matrix
10:         Build and store new error matrix
11:                              ▷ F_i^p is from ith last cycle
12:         if Current cycle < l then
13:                 ▷ Number of stored Fock matrices = l
14:             F' = (X^p)^T F^p X^p
15:         else
16:             Solve DIIS matrix
17:                                  ▷ DIIS coefficients → c_i
18:             F' = (X^p)^T (Σ_{i=1}^{l} c_i F_i^p) X^p
19:         end if
20:         Diagonalise F'              ▷ Eigenvectors → C'
21:         C^p = X^p C'
22:     end for
23:     if not all domains have converged then
24:         SCF_CYCLE                          ▷ Recursive call
25:     end if
26: end procedure
```

Algorithm 8. Chem1D overview

```
1:  procedure CHEM1D(input)
2:      Read input
3:      Allocate integral storage
4:      for p ∈ 𝒟 do     ▷ Build the one-electron matrices
5:          OVERLAP(p)
6:          KINETIC(p)
7:          POTENTIAL(p)
8:      end for
9:      ERI          ▷ Build the set of two-electron integrals
10:     DOUBLE_BAR       ▷ Contract the quasi-integrals
11:     for p ∈ 𝒟 do
12:                 ▷ Build the orthogonalisation matrices
13:         BUILD_X(p)
14:     end for
15:     SCF_CYCLE
16:     MO_TRANSFORM
17:      ▷ Transform the double-bar integrals to MO basis
18:     MPN_CORRELATION
19:     Print output
20: end procedure
```

3.4. *Pseudocode overview*

Now that we have defined how the various components operate, we present an overview of the main CHEM1D program in Algorithm 8.

4. Results

4.1. *Atomic energies*

We begin our tests of CHEM1D by studying atomic systems. In our earlier work [28], we computed the total energies, ionisation energies and electron affinities of the first 10 elements very accurately. As a preliminary demonstration of the capabilities of CHEM1D, we have performed the same study here.

Our experiments suggest that a basis set of nine exponential functions on each side of the nucleus (see Equations (1) and (2)) produces the best results for this study. CHEM1D's default value of $\alpha = Z/m^2$ has been used, where $m = 9$ and Z is the charge of the atom's nucleus. We remove one column from the orthogonalisation matrix to facilitate convergence and the results are shown in Table 1.

For small atoms, the total energies produced by CHEM1D compare favourably with our previous results. Up to boron, the Hartree–Fock energies agree with our previous results within a millihartree. However, beyond this point, the results diverge significantly. These inaccuracies stem directly from the lack of diffuse functions in the basis set that we have used in this study. Our previous results showed that heavy atoms in 1D are surprisingly diffuse objects [28]. This error is most evident in the ionisation energy and electron affinity of fluorine, where the constriction imposed by the poor basis set is great enough to reverse the sign of these quantities.

Unsurprisingly, the Møller–Plesset correlation energies also suffer from basis set incompleteness because, as the number of electrons increases, the virtual space is progressively diminished.

The total energy errors are inherited by the ionisation energies and electron affinities and, as before, the lack of diffuse functions is to blame.

In spite of the basis set deficiencies, we are still able to observe some of the unusual properties of 1D atoms. In particular, we are able to reconstruct the thin periodic table presented in our previous work by looking at the periodic behaviour of the ionisation energies. In 3D chemistry, the ionisation energy increases monotonically when moving across a row of the periodic table before dropping when moving to the next row. We find similar behaviour here. The period of these trends is only two atoms however, which suggests that the periodic table of 1D elements has only two groups.

4.2. *Diatomic molecules*

We now turn our attention to diatomic molecules. Our previous study [28] investigated diatomics with a maximum of

Table 1. Atomic energies (in hartrees), ionisation energies and electron affinities (in electron volts).

	Atomic energies			Ionisation energies			Electron affinities		
Atom	$-E_{HF}$	$-E_{MP2}$	$-E_{MP3}$	HF	MP2	MP3	HF	MP2	MP3
H	0.500000	0.000	0.000	13.606	13.606	13.606	3.887	3.933	3.956
He	3.242552	1.998	2.636	33.812	33.866	33.883			
Li	8.007278	2.953	3.644	4.485	4.507	4.512	1.396	1.409	1.414
Be	15.415561	5.128	6.127	10.351	10.388	10.397			
B	25.356662	6.818	8.036	2.060	2.077	2.084	0.584	0.594	0.598
C	38.082819	9.613	11.420	4.621	4.654	4.666			
N	53.558680	11.175	12.967	1.054	1.056	1.057	0.349	0.350	0.351
O	71.890505	13.173	15.187	2.232	2.241	2.244			
F	93.055546	14.728	16.757	−0.208	−0.222	−0.227	−1.277	−1.294	−1.301
Ne	117.240157	14.951	16.670	1.075	1.069	1.067			

The electron affinities for He, Be, C, O and Ne have been omitted. It has been found previously that the anions of these species are auto-ionising [28].

two electrons. We concluded that having two or more electrons in a finite domain is highly destabilising because of the large resulting kinetic energy. We also observed that atomic species with an odd number of electrons carry a permanent dipole due to the particle impenetrability trapping different numbers of electrons on each side of the nucleus. We speculated that, as a consequence of this, stable molecules could form with multiple electrons in a finite domain, despite the increase in kinetic energy, due to favourable dipole–dipole interactions. Thanks to the recent developments in CHEM1D we are now able to test this conjecture.

Results for a small collection of diatomic molecules can be found in Table 2. Only electronic configurations which permit a bound molecule have been included. We use a basis set of eight exponential functions in each infinite domain and a combination of six even and six odd functions in the finite domain.

These results show some interesting effects which reveal that our earlier prediction was not entirely accurate. In fact, there are a number of striking results which are counter-intuitive from the viewpoint of 3D chemistry.

First, we see that H has at least one favourable bonding configuration with other nuclei. The reason for this is simple: H can present an unshielded positive charge to the electrons of the other nucleus. This allows it to bind strongly even to the 1D elements with no permanent dipole. In fact, the bonding in $_1H_2Be_2$ is stronger than that of $_1H_1He_1$. The H nucleus interacts with the outermost electron of the other atom, which in the case of Be is shielded from the charge of its own nucleus by the interior electron.

There are three configurations for LiH in 1D that seem likely to result in bonding: $_1Li_2H_1$, $_2Li_2H$ and $_2Li_1H_1$. The last of these does not result in binding, probably because the opposed dipoles of the H and Li atoms result in insufficient stabilising potential energy. The other two do form a bound molecule, although there is a very large difference in binding energy. The comparatively small bond dissociation energy of $_2Li_2H$ is a result of the second exterior electron being forced into a higher energy orbital; in $_1Li_2H_1$, both electrons on the outside of the molecule are able to occupy the lowest energy orbital in their domain.

The final noteworthy result relating to the binding in hydrogen-containing diatomics is the remarkable strength of the bond with respect to its length (except in H_2Li_2). We noted in our previous manuscript that the length of the H_1H_1 bond is roughly double than that of the 3D H_2 molecule, while they have a similar strength [28,48]. The bond in $_1H_2Li_1$ however is roughly 90% of the strength of the bond

Table 2. Equilibrium bond distances (in bohrs, Hartree–Fock energies (in hartrees), correlation energies (in millihartrees) and bond dissociation energies (in hartrees) of bound states of diatomic molecules.

					Bond dissociation energies		
Molecule	R_{eq}	$-E_{HF}$	$-E_{MP2}$	$-E_{MP3}$	HF	MP2	MP3
H_1H_1	2.636	1.184572	0.844	1.154	0.185	0.185	0.186
$_1H_1He_1$	2.025	3.880304	2.300	2.978	0.138	0.138	0.138
$_1H_2Li_1$	5.076	8.679540	4.507	5.747	0.172	0.174	0.174
H_2Li_2	5.212	8.541236	3.565	4.352	0.034	0.035	0.035
$_1H_2Be_2$	3.895	16.074792	6.859	8.291	0.159	0.161	0.161
$_1He_2Li_2$	4.505	11.258911	5.398	6.757	0.009	0.010	0.010
$_1Li_3Li_2$	7.142	16.021014	7.107	8.694	0.006	0.008	0.008

in H_1H_1, yet the bond is almost double the length. This is also much longer than the corresponding 3D bond length, approximately 3.015 bohrs [49]. The strength of the 3D LiH bond falls between the two bound configurations of 1D LiH at approximately 92 millihartrees [49], making the bond in the more favourable $_1H_2Li_1$ configuration significantly stronger than its 3D counterpart.

Diatomics of two heavy atoms produce more interesting and unexpected results, while also revealing a deficiency in CHEM1D.

We find that the molecule $_1He_2Li_2$ is very gently bound. Previously, we would have expected this molecule to be unbound given the lack of stabilising dipole interactions. Given the bonding behaviour of the $_1H_1He_1$ and $_1H_2Be_2$ molecules however, we might have expected this bond to be reasonably strong as a result of similar electrostatic arguments. When the H atom is replaced by Li, we introduce an extra electron into the finite bond. Now that the domain contains two electrons, one is forced to occupy a higher energy orbital. This carries a significant energy penalty which the favourable electrostatic interactions are only just able to overcome.

We examined two possible configurations of the Li dimer: $_2Li_2Li_2$ and $_1Li_3Li_2$. The former configuration does not bind due to the opposition of the dipoles on the two individual atoms. The latter configuration does bind however, but with an extremely long bond length. Using CHEM1D to determine the bonding energy suggests that this molecule has a lower binding energy than $_1He_2Li_2$. This is unexpected given the dipole–dipole interactions that should stabilise the Li dimer.

We have also examined this using a quadruple-precision version of CHEM1D. Using higher precision allows us to use larger basis sets before near linear dependence becomes an issue. The results from this program suggest that the equilibrium bond length is significantly longer (at least 8.5 bohrs). Around this configuration the binding energy increases by at least 40 millihartrees, which suggests the relative bonding behaviour we expect is more likely.

This would give 1D $_1Li_3Li_2$ a dissociation energy close to that of the 3D Li_2 dimer (approximately 39 millihartrees [50]). Like the 1D hydrogen molecule however, the 1D lithium dimer has a significantly longer bond than the 3D dimer, 7.142 bohrs for the 1D molecule compared to approximately 5.051 bohrs for the 3D molecule [50].

Unfortunately, the basis sets that can typically be used in double precision without incurring numerical problems have only limited ability to describe long bonds with multiple electrons. The basis functions we have used are high in amplitude around the middle of the bond and decay relatively quickly towards its edges. In a stretched bond, however, the electrons tend to localise near the nuclei; in a bond with many electrons and accordingly heavy nuclei, this localisation rapidly becomes very restrictive. Describing these orbitals, which are built up near the edges of the bond, with the basis sets we have described requires large molecular orbital coefficients with oscillating signs.

In light of this, we have refrained from examining further systems containing three or more electrons in a finite domain. Additionally, we consider that a bond length of more than 6 bohrs is likely to be indicative of a significant drop in numerical accuracy.

4.3. Triatomic molecules

In addition to diatomics, we have also examined a small selection of triatomic molecules. We have used the same methods as were employed for the diatomic molecules. The results can be seen in Table 3.

When compared to the behaviour of the diatomic molecules, this set of results reveals a great deal about how larger molecules are likely to form in 1D. The atomisation energies of each triatomic is roughly equal to the sum of the bond dissociation energies in the appropriate two diatomic molecules. The difference can be rationalised as a consequence of the alignment of the permanent dipoles belonging to the constituent atoms.

Taking $H_1H_1H_1$ as a simple example, we obtain an approximate atomisation energy of 0.370 hartrees by doubling the bond dissociation energy of H_1H_1. The dipoles of all three atoms are aligned however, and as a result there is a bonus to the binding strength of about 15 millihartrees, giving a final atomisation energy of approximately 0.385.

Table 3. Equilibrium bond distances (in bohrs), Hartree–Fock energies (in hartrees), correlation energies (in millihartrees) and atomisation energies (in hartrees) of triatomic molecules.

						Atomisation energies		
Molecule	R_{eq}		$-E_{HF}$	$-E_{MP2}$	$-E_{MP3}$	HF	MP2	MP3
$H_1H_1H_1$	2.648	2.762	1.883315	1.538	2.099	0.383	0.385	0.385
$_1H_1H_1He_1$	2.705	2.033	4.565870	3.068	4.037	0.323	0.324	0.325
$_1H_1He_1H_1$	2.031	2.031	4.493606	2.637	3.417	0.251	0.252	0.252
$_1H_1H_2Be_2$	2.388	4.426	16.841024	6.985	8.480	0.425	0.427	0.428
$_1H_2Be_2H_1$	3.881	3.881	16.730968	8.060	9.862	0.315	0.318	0.319
$_1Li_2H_2Li_2$	4.129	8.458	16.766343	7.902	9.755	0.252	0.254	0.254

Moving down the set of examples, we find that the atomisation energy of $_1H_1H_1He_1$ is almost exactly equal to the strength of its two constituent bonds. The alignment of the two hydrogen dipoles is already accounted for in the bond dissociation energy of H_1H_1, and the helium atom lacks a dipole which would provide an extra contribution. The strength of the binding in $_1H_1He_1H_1$ (approximately 0.25 hartrees) is slightly lower than that of two $_1H_1He_1$ bonds (approximately 0.275 hartrees) due to the repulsion of the opposing hydrogen dipoles.

This destabilisation is dependent upon the distance between the two interacting dipoles. We see a loss of approximately 25 millihartrees in the bonding strength of $_1H_1He_1H_1$, but in $_1H_2Be_2H_1$, where the distance between the two hydrogen atoms has almost doubled, a loss of only approximately 5 millihartrees is observed. Additionally, the magnitude of the effect is dependent upon the types of dipoles interacting. As mentioned above, the $H_1H_1H_1$ molecule gains roughly 15 millihartrees from the additional dipole interaction, while $_1Li_2H_2Li_2$ gains approximately 50 millihartrees from the interaction between the two Li atoms.

It should be noted that this gain may actually be underestimated by our calculations due to the large equilibrium bond length we find in this molecule. As stated in Section 4.2, we believe that our basis set is insufficient for accurately describing bonds with lengths above 6 bohrs. It appears that the bonds in triatomic molecules are noticeably longer than those in diatomics, even when favourable dipole interactions increase the strength of the molecule's bonds. This leads to very long bond lengths for Li containing molecules, and due to concerns of numerical accuracy we have omitted results for other Li containing triatomic molecules.

5. Conclusion

We have written a program, called CHEM1D, for computing energies of 1D molecules at the Hartree–Fock level and beyond. This has enabled us to probe the behaviour of 1D molecules that were previously unaccessible, and to develop a more sophisticated understanding of 1D chemistry.

In particular, we have shown that multi-electron bonds do exist in 1D molecules, notwithstanding our previous conjecture to the contrary. We have also observed some strange effects that result from the limited dimensionality of the system, such as unusual strong bonding between distant atoms and the dominance of permanent dipoles upon reactivity.

Our experiments have highlighted some of the current limitations of the CHEM1D program and, in particular, it appears that our choice of basis functions is non-optimal. This presents avenues for continued development that we plan to pursue in order to allow the examination of more complicated 1D systems.

The CHEM1D package can be freely downloaded from the *Molecular Physics* webpage.

Acknowledgements

We thank Dr Pierre-François Loos for many helpful discussions.

Disclosure statement

No potential conflict of interest was reported by the authors.

Funding

Caleb J. Ball is grateful for an Australian Postgraduate Award. Peter M.W. Gill thanks the NCI National Facility for generous grants of supercomputer time and the Australian Research Council for funding [grant number DP120104740], [grant number DP140104071].

References

[1] R. Saito, G. Dresselhauss, and M.S. Dresselhaus, *Properties of Carbon Nanotubes* (Imperial College Press, London, 1998).
[2] R. Egger and A.O. Gogolin, Eur. Phys. J. B **3**, 281 (1998).
[3] M. Bockrath, D.H. Cobden, J. Lu, A.G. Rinzler, R.E. Smalley, L. Balents, and P.L. McEuen, Nature **397**, 598 (1999).
[4] H. Ishii, H. Kataura, H. Shiozawa, H. Yoshioka, H. Otsubo, Y. Takayama, T. Miyahara, S. Suzuki, Y. Achiba, M. Nakatake, T. Narimura, M. Higashiguchi, K. Shimada, H. Namatame, and M. Taniguchi, Nature **426**, 540 (2003).
[5] M. Shiraishi and M. Ata, Solid State Commun. **127**, 215 (2003).
[6] A. Schwartz, M. Dressel, G. Grüner, V. Vescoli, L. Degiorgi, and T. Giamarchi, Phys. Rev. B **58**, 1261 (1998).
[7] V. Vescoli, F. Zwick, W. Henderson, L. Degiorgi, M. Grioni, G. Gruner, and L.K. Montgomery, Eur. Phys. J. B **13**, 503 (2000).
[8] T. Lorenz, M. Hofmann, M. Grüninger, A. Freimuth, G.S. Uhrig, M. Dumm, and M. Dressel, Nature **418**, 614 (2002).
[9] M. Dressel, K. Petukhov, B. Salameh, P. Zornoza, and T. Giamarchi, Phys. Rev. B **71**, 075104 (2005).
[10] T. Ito, A. Chainani, T. Haruna, K. Kanai, T. Yokoya, S. Shin, and R. Kato, Phys. Rev. Lett. **95**, 246402 (2005).
[11] F.P. Milliken, C.P. Umbach, and R.A. Webb, Solid State Commun. **97**, 309 (1996).
[12] S.S. Mandal and J.K. Jain, Solid State Commun. **118**, 503 (2001).
[13] A.M. Chang, Rev. Mod. Phys. **75**, 1449 (2003).
[14] A.R. Goñi, A. Pinczuk, J.S. Weiner, J.M. Calleja, B.S. Dennis, L.N. Pfeiffer, and K.W. West, Phys. Rev. Lett. **67**, 3298 (1991).
[15] O.M. Auslaender, A. Yacoby, R. dePicciotto, K.W. Baldwin, L.N. Pfeiffer, and K.W. West, Phys. Rev. Lett. **84**, 1764 (2000).
[16] S.V. Zaitsev-Zotov, Y.A. Kumzerov, Y.A. Firsov, and P. Monceau, J. Phys. **12**, L303 (2000).
[17] F. Liu, M. Bao, K.L. Wang, C. Li, B. Lei, and C. Zhou, Appl. Phys. Lett. **86**, 213101 (2005).
[18] H. Steinberg, O.M. Auslaender, A. Yacoby, J. Qian, G.A. Fiete, Y. Tserkovnyak, B.I. Halperin, K.W. Baldwin, L.N. Pfeiffer, and K.W. West, Phys. Rev. B **73**, 113307 (2006).
[19] H. Monien, M. Linn, and N. Elstner, Phys. Rev. A **58**, R3395 (1998).

[20] A. Recati, P.O. Fedichev, W. Zwerger, and P. Zoller, J. Opt. B. Opt. **5**, S55 (2003).
[21] H. Moritz, T. Stoferle, K. Guenter, M. Kohl, and T. Esslinger, Phys. Rev. Lett. **94**, 210401 (2005).
[22] L.O. Wagner, E. Stoudenmire, K. Burke, and S.R. White, Phys. Chem. Chem. Phys. **14**, 8581 (2012).
[23] E.M. Stoudenmire, L.O. Wagner, S.R. White, and K. Burke, Phys. Rev. Lett. **109**, 056402 (2012).
[24] D.J. Doren and D.R. Herschbach, Chem. Phys. Lett. **118**, 115 (1985).
[25] J.G. Loeser and D.R. Herschbach, J. Chem. Phys. **84**, 3882 (1986).
[26] J.G. Loeser and D.R. Herschbach, J. Chem. Phys. **84**, 3893 (1986).
[27] A. López-Castillo, Chaos **18** (3), 033130 (2008).
[28] P.F. Loos, C.J. Ball, and P.M.W. Gill, Phys. Chem. Chem. Phys. **17**, 3196 (2015).
[29] R. Loudon, Am. J. Phys. **27**, 649 (1959).
[30] T.D. Imbo and U.P. Sukhatme, Phys. Rev. Lett. **54**, 2184 (1985).
[31] H.N. Núñez-Yépez and A.L.S. Brito, Eur. J. Phys. **8**, 307 (1987).
[32] H.N. Núñez-Yépez, C.A. Varga, and A.L. Salas-Brito, Phys. Rev. A **39**, 4306 (1989).
[33] M. Moshinsky, J. Phys. A **26**, 2445 (1993).
[34] R.G. Newton, J. Phys. A **27**, 4717 (1994).
[35] D. Xianxi, J. Dai, and J. Dai, Phys. Rev. A **55**, 2617 (1997).
[36] K. Connolly and D.J. Griffiths, Am. J. Phys. **75**, 524 (2007).
[37] T. Kato, Trans. Am. Math. Soc. **70**, 212 (1951).
[38] C.R. de Oliveira and A.A. Verri, Ann. Phys. **324**, 251 (2009).
[39] C.R. de Oliveira, Phys. Lett. A **374**, 2805 (2010).
[40] C.R. de Oliveira and A.A. Verri, J. Math. Phys. **53**, 052104 (2012).
[41] H.N. Núñez-Yépez, A.L. Salas-Brito, and D.A. Solis, Phys. Rev. A **83**, 064101 (2011).
[42] H.N. Núñez-Yépez, A.L. Salas-Brito, and D.A. Solis, Phys. Rev. A **89**, 049908(E) (2014).
[43] A. Szabo and N.S. Ostlund, *Modern Quantum Chemistry* (McGraw-Hill, New York, 1989).
[44] F.W.J. Olver, D.W. Lozier, R.F. Boisvert and C.W. Clark, editors, *NIST Handbook of Mathematical Functions* (Cambridge University Press, New York, 2010).
[45] Wolfram Research, Inc., *Mathematica*, Version 9.0 (Wolfram Research, Inc., Champaign, Illinois, 2012).
[46] P. Pulay, Chem. Phys. Lett. **73** (2), 393–398 (1980).
[47] P. Pulay, J. Comp. Chem. **3** (4), 556–560 (1982).
[48] W. Kolos and L. Wolniewicz, J. Chem. Phys. **49**, 404 (1968).
[49] W.C. Stwalley and W.T. Zemke, J. Phys. Chem. Ref. Data **22** (1), 87–112 (1993).
[50] R.J. Le Roy, N.S. Dattani, J.A. Coxon, A.J. Ross, P. Crozet, and C. Linton, J. Chem. Phys. **131** (20), 204309-1–204309-13 (2009).